Atmos. Meas. Tech. Discuss., 8, 8157–8189, 2015
www.atmos-meas-tech-discuss.net/8/8157/2015/
doi:10.5194/amtd-8-8157-2015

Atmospheric Measurement Techniques Discussions
Open Access

Intercomparison of snowfall estimates derived from the CloudSat Cloud Profiling Radar and the ground based weather radar network over Sweden

L. Norin[1], A. Devasthale[1], T. S. L'Ecuyer[2], N. B. Wood[3], and M. Smalley[2]

[1]Atmospheric Remote Sensing Unit, Research Department, Swedish Meteorological and Hydrological Institute, Norrköping, Sweden
[2]Department of Atmospheric and Oceanic Sciences, University of Wisconsin-Madison, Madison, Wisconsin, USA
[3]Cooperative Institute for Meteorological Satellite Studies, University of Wisconsin-Madison, Madison, Wisconsin, USA

Received: 10 July 2015 – Accepted: 14 July 2015 – Published: 6 August 2015

Correspondence to: L. Norin (lars.norin@smhi.se)

Published by Copernicus Publications on behalf of the European Geosciences Union.

Abstract

To be able to estimate snowfall accurately is important for both weather and climate applications. Ground-based weather radars and space-based satellite sensors are often used as viable alternatives to rain-gauges to estimate precipitation in this context. The Cloud Profiling Radar (CPR) onboard CloudSat is especially proving to be a useful tool to map snowfall globally, in part due to its high sensitivity to light precipitation and ability to provide near-global vertical structure. The importance of having snowfall estimates from CloudSat/CPR further increases in the high latitude regions as other ground-based observations become sparse and passive satellite sensors suffer from inherent limitations.

Here we intercompared snowfall estimates from two observing systems, CloudSat and Swerad, the Swedish national weather radar network. Swerad offers one of the best calibrated data sets of precipitation amount at very high latitudes that are anchored to rain-gauges and that can be exploited to evaluate usefulness of CloudSat/CPR snowfall estimates in the polar regions. In total 7.2×10^5 matchups of CloudSat and Swerad over Sweden were inter-compared covering all but summer months (October to May) from 2008 to 2010. The intercomparison shows encouraging agreement between these two observing systems despite their different sensitivities and user applications. The best agreement is observed when CloudSat passes close to a Swerad station (46–82 km), when the observational conditions for both systems are comparable. Larger disagreements outside this range suggest that both platforms have difficulty with shallow snow but for different reasons. The correlation between Swerad and CloudSat degrades with increasing distance from the nearest Swerad station as Swerad's sensitivity decreases as a function of distance and Swerad also tends to overshoots low level precipitating systems further away from the station, leading to underestimation of snowfall rate and occasionally missing the precipitation altogether. Further investigations of various statistical metrics, such as the probability of detection, false alarm rate, hit rate, and the Hanssen–Kuipers skill scores, and the sensitivity of

these metrics to snowfall rate and the distance from the radar station, were carried out. The results of these investigations highlight the strengths and the limitations of both observing systems at the lower and upper ends of snowfall distributions and the range of uncertainties that could be expected from these systems in the high latitude regions.

1 Introduction

Snowfall is a crucial component of the Earth's water and energy cycle (Levizzani et al., 2011; Waliser et al., 2011). Its effect on weather and climate are multi-faceted over high latitude regions. At shorter time scales ranging from days to months, snowfall can readily change the surface temperature, impact atmospheric dynamics, and influence circulation patterns. Accurate representation of snowfall is one of the key challenges confronted by forecasting and numerical weather prediction models. Characterising snowfall at sub-daily to daily scales is of great societal value. For example, heavy snowfall caused by a convective snow-band event can completely blanket the transportation infrastructure leading to traffic chaos. So for high-latitude countries like Sweden, the timely information on snowfall helps in planning daily communal services as well as to better manage tourism and agricultural industries. Ground-based weather radars are most commonly used to monitor precipitation for such weather applications.

From the climate perspective, better understanding of snowfall is also warranted (Waliser et al., 2011). For example, variability in snowfall directly influences variability in surface albedo and temperature and thus has profound impact on the radiation balance. Snow cover also impacts surface-air interactions by regulating heat and mass exchanges. Snowfall further has far-reaching impacts via teleconnections. For example, variability in Eurasian snow cover is shown to influence Asian monsoon rainfall (Liu and Yanai, 2002). Even the changes in snow cover onset over Siberia is said to influence Southeast Asian monsoon rainfall (Ye et al., 2005). Other studies argue that the increased snowfall over Himalayas has negative impact on Indian monsoon rainfall (Turner and Slingo, 2011), mainly due to increased reflection and cooling of the sur-

AMTD
8, 8157–8189, 2015

face leading to weakened land-sea thermal contrast which is considered an important trigger for the strength of monsoonal circulation. During spring, melting snow regulates the surface and river run-off in a catchment. Therefore, the long-term changes in snowfall characteristics directly impact the hydrological cycle at a regional scale. Space based remote sensing is often used either as a viable alternative or in combination with ground-based measurements to monitor precipitation for climate applications.

In spite of its importance mentioned above, characterising snowfall globally has been difficult either due to the absence or limited coverage or of limited capabilities of the observing systems. In-situ measurements from precipitation-gauges provide invaluable data, but they are mainly restricted to land areas and are geographically inhomogeneous and sparse especially over the high latitude regions. Apart from networks of ground based weather radars covering very small geographical areas in both hemispheres, a reliable source of snowfall information over the high latitudes and the polar regions (where snowfall matters most) is generally lacking. Space based observation of snowfall is, in a broader sense, in its infancy. The satellite sensors that operate at microwave or millimetre wavelengths are showing promise to obtain quantitatively reliable estimates (Noh et al., 2009; Surussavadee and Staelin, 2009; Levizzani et al., 2011; Liu and Seo, 2013), but they are still of inadequate quality over the high latitudes, especially over land and ice covered surfaces. The optical imaging sensors do provide information on the snow cover extent but the critical information on snowfall rate still remains illusive. This is however changing since the launch of CloudSat as a part of the A-Train convoy of satellites in 2006 (L'Ecuyer and Jiang, 2010). For the first time, the active Cloud Profiling Radar (CPR) onboard CloudSat offers a possibility of obtaining realistic estimates of snowfall rate from the space (Liu, 2008; Kulie and Bennartz, 2009; Wood, 2011; Wood et al., 2013).

As every observing system has its strengths and weaknesses, the estimates of snowfall from both the CloudSat/CPR and ground-based weather radar systems could be further improved if the synergy of these platforms could be exploited (Cao et al., 2014; Smalley et al., 2014). With their better spatial and temporal resolution and an-

AMTD
8, 8157–8189, 2015
Intercomparison of snowfall
L. Norin et al.

chorage to high quality rain-gauges, weather radars offer an independent source of information to intercompare snowfall estimates from the CloudSat/CPR. The snowfall estimates from CloudSat/CPR, unlike those from weather radars, are uniformly calibrated and generally insensitive to the vertical location of the precipitating system. Furthermore, the weather radar beams overshoot very low precipitating systems, missing them as the observation distance from the radar increases. But the lowermost few bins of CloudSat, ranging roughly from 600 to 1200 m in height, are also affected by ground clutter (so-called radar blind-zone) and could lead to an underestimation of reflectivity and precipitation amount at the surface (Maahn et al., 2014). With regard to detectability, CloudSat is about an order of magnitude more sensitive to very light precipitation than any other existing space based sensor (Skofronick-Jackson et al., 2012). On the other hand, unlike weather radars, CloudSat reflectivities can saturate in case of heavy snowfall events (Cao et al., 2014). All of these considerations suggest that quantifying the strengths and weaknesses of these two observing systems (i.e. CloudSat/CPR and ground based weather radars) would not only be beneficial to improve their snowfall estimates, but would also help in bracketing the spread in their expected uncertainties. Such knowledge could certainly help in evaluating snowfall variability simulated by climate models.

With that in mind, the main focus of the present study is to quantitatively intercompare snowfall estimates from these two observing systems over Sweden. The Swedish radar network has been operational since the 1980s and more than a decade of archived precipitation data exist to inter-compare with space based estimates (Michelson et al., 2000; Michelson and Koistinen, 2002; Michelson, 2006; Devasthale and Norin, 2014). Apart from offering an independent source of snowfall estimates, the high latitude geographical position of the Swedish radars entails sampling of different meteorological regimes under which CloudSat/CPR data could be intercompared. The next section provides an overview of CloudSat/CPR and weather radar data sets followed by the description of results in the third section. The results are summarised in the final section.

2 Data sets and processing

2.1 Snowfall product 2C-SNOW-PROFILE from CloudSat

CloudSat snowfall estimates were obtained from the 2C-SNOW-PROFILE data product, release R04 (Wood, 2011; Wood et al., 2013). This product uses a Bayesian optimal estimation retrieval algorithm (Rodgers, 2000) to estimate vertically-resolved properties of snowfall from vertical profiles of W-band (94 GHz) reflectivities measured by CloudSat's Cloud Profiling Radar (CPR). The CloudSat orbit is such that the radar makes observations between 82° N and 82° S latitude, completing one orbit approximately every 99 min (Tanelli et al., 2008) and repeating its orbital ground track every 16 days. This orbit leads to moderately dense spatial sampling at high latitudes. Profiles have a horizontal spatial resolution of 1.7 km along-track by 1.4 km cross-track. The radar has an intrinsic vertical resolution of 485 m, but measurements are oversampled to provide an effective vertical resolution of 239 m.

Rather than assuming a fixed relationship between reflectivity and snowfall rate (a so-called Z–S relationship), the 2C-SNOW-PROFILE retrieval algorithm estimates vertical profiles of the probability density functions (PDFs) of snow particle size distribution parameters. These posterior PDFs are estimated by minimizing a cost function that incorporates a priori estimates of the environmental distributions of these parameters as well as uncertainty-weighted differences between the observed and forward-modelled radar reflectivity profile. The reflectivity forward model uses high-quality descriptions of the PDFs of snow particle microphysical and scattering properties as functions of size (Wood et al., 2015) as well as treatments for attenuation and multiple scattering by snow particles. The estimates of the size distribution parameters are then used along with the forward model's microphysical properties to construct the vertically-resolved PDFs of snowfall rate and other snow properties.

A retrieval is performed if the 2C-PRECIP-COLUMN product (Haynes et al., 2009) has categorized the surface precipitation as snow or as mixed-phase with a melted mass fraction of less than 10 %. The melted mass fraction is estimated based on the

AMTD
8, 8157–8189, 2015

height of the freezing level and assumptions about the environmental lapse rate below the freezing level. Temperature information is obtained from reanalysis products of the European Centre for Medium-range Weather Forecasting co-located to the CloudSat profile.

The surface snowfall rate is estimated from the retrieved profile of snowfall rates. Ground clutter affects the CPR measurements in the radar range bins nearest the surface. Because of this, these near-surface bins cannot be included in the reflectivity profiles when retrievals are performed, creating what is sometimes called a blind zone. Over land, this zone extends about 1 km above the surface. Consequently, the approach taken currently by 2C-SNOW-PROFILE is to estimate the surface snowfall rate as the rate retrieved in the radar bin immediately above the blind zone. This surface snowfall rate is assigned a confidence value from "None" to "High" depending on the expected performance of the forward model and the reliability of the temperature-based estimate of the precipitation phase, among other factors.

2.2 Snowfall product based on the Swedish weather radar network

The Swedish national weather service has 12 horizontally polarised C-band Doppler radars which together form the Swedish weather radar network. The enhanced sensitivity of C-band radars compared to S-band radars makes the Swedish radar network particularly well-suited for snowfall studies. These radars measure three spectral moments: the radar reflectivity factor (hereafter referred to as reflectivity, Z), radial velocity, and spectrum width. From these moments quantities such as precipitation rate, wind speed, and turbulence are estimated. In this work we focus only on reflectivity as our main interest is the snowfall rate.

Reflectivity, Z, measures the fraction of returned power, and is interpreted in terms of the backscattering characteristics of the observed particles. The radars measure reflectivities between $-30 \leq Z \leq 71.6$ dBZ in steps of 0.4 dBZ. The minimum reflectivity value, Z_{min}, is assigned to all measurements ranging from $-\infty$ to -30 dBZ. Such measurements are referred to as undetected measurements and are interpreted by the

Discussion Paper | Discussion Paper | Discussion Paper | Discussion Paper |
AMTD
8, 8157–8189, 2015
Intercomparison of snowfall
L. Norin et al.

radar as clear conditions. As the strength of an echo decreases with the square of its distance, further from the radars the upper limit of $Z_{\min}$ increases (see, e.g., Doviak and Zrnić, 2006).

To suppress ground echoes, the Swedish weather radars are equipped with clutter filters. The clutter filters work by omitting the amplitudes of the three frequency channels closest to zero in the frequency spectrum, suppressing echoes with radial velocities less than $\pm 1\,\mathrm{m\,s^{-1}}$. The radar receiver is protected from overload by damping nearby signals by 60 dB, making data from the first 4 km from the radar unusable.

The scan strategy of the Swedish radars consists of performing azimuthal scans around a vertical axis for 10 different tilt angles, θ. The lowest scan is made at $\theta = 0.5^\circ$ and the highest is made at $\theta = 40^\circ$. These scans, which together make up a polar volume data set, are repeated every 15 min. Relevant radar characteristics are summarised in Table 1.

From polar volume data sets horizontal cross sections of radar reflectivity at a certain altitude can be generated. Over areas where no data exist at the specified altitude the measurement nearest in height is selected. Such cross sections are referred to as pseudo-constant altitude plan position indicator (PCAPPI). In Sweden, the PCAPPIs are defined at 500 m altitude above the corresponding radar.

Nordrad (Carlsson, 1995) is a close collaboration among the Swedish Meteorological and Hydrological Institute (SMHI), the Norwegian Meteorological Institute, the Finnish Meteorological Institute, the Estonian Meteorological and Hydrological Institute, and the Latvian Environment, Geology and Meteorology Agency. An additional agreement exists with the Danish Meteorological Institute. Within the Nordrad collaboration radar PCAPPIs are exchanged in real time. All together, there are currently 35 weather radars operating in Sweden, Norway, Finland, Estonia, Latvia, and Denmark.

At the SMHI, composite radar images over the Nordic countries are generated using PCAPPI data from as many available weather radars as possible. Before merging the PCAPPIs into a composite image some quality adjustments are made. Radar measurements may be affected by nearby obstacles such as trees or mountains. A beam

AMTD
8, 8157–8189, 2015

blockage correction, based on the method by Bech et al. (2003), is applied to correct for the reduction in reflectivity due to topography. Radar measurements may also contain echoes from non-precipitating objects such as ground clutter or clear air targets. Non-precipitation echoes are removed by a filter using satellite observations. Radar echoes from areas which are classified as cloud free by the satellite are removed by the filter (Michelson, 2006).

Due to a combination of the positive non-zero angle of the lowest scan and the curvature of the Earth's surface, measurements at increasing distances from the radars correspond to increasing heights (with increasing risk of completely or partially overshooting precipitating clouds), see e.g. Fig. 2. As a result, precipitation estimates at large distances from the radar may be of lower quality than those within 100 km from the radar. In order to correct for this distance dependence data from rain gauges, which are considered to measure precipitation accurately, are used to calibrate the PCAPPIs. In order to compare radar reflectivities to the rain gauge-measured precipitation the reflectivities are converted to precipitation rate R (mm h^{-1}) using the empirical relationship $Z = aR^b$, where $a = 200$ and $b = 1.5$ (see, e.g. Battan, 1973).

The radar data is adjusted by fitting a second degree polynomial to the logarithmic gauge-to-radar ratio, as a function of distance to the nearest radar. Radar measurements above 0.1 mm and rain gauge measurements above 0.5 mm from one week worth of time are used in the calculations. The gauge adjustment method is described in detail in Michelson and Koistinen (2002). The quality adjusted PCAPPIs are used to produce a composite image, Nordrad, covering the Nordic countries. The Nordrad composite image has a spatial resolution of 2 km × 2 km and is generated every 15 min.

A simple but robust snowfall product was generated by combining Nordrad's precipitation composite with 2 m temperatures from MESAN, a system for operational mesoscale univariate analyses of selected meteorological parameters (Häggmark et al., 2000). The model domain of MESAN covers Scandinavia and the entire drainage basin of the Baltic Sea. The analysis is performed on a rotated latitude–longitude grid with a spatial resolution of 0.1° (11 km) and a time resolution of one hour. For every

Nordrad composite image the 2 m temperature field from MESAN nearest in time and space was used to generate a snowfall product. If the 2 m temperature was less than or equal to zero degrees Celsius the corresponding precipitation from Nordrad was classified as snow, otherwise as rain.

In this work we have used snowfall estimates from the Nordrad composites but only selected measurements originating from the area covered by Swedish radars. For the purpose of this paper we call this selection of data Swerad. Figure 1 shows the area covered by Nordrad and Swerad together with the location of all radars as well as the selected tracks of CloudSat.

2.3 Processing

During 2007 a modification was made to the Swedish radar hardware to implement Doppler processing for all scans. In order to have a homogeneous data set we have therefore only used radar data collected after 1 January 2008, even though CloudSat was launched in 2006. For the present study, we used all ascending and descending passes of CloudSat (except during summer months, June to September) from 1 January 2008 to 31 December 2010 between 54 and 70° N latitude band. In total, we analysed 1143 number of tracks and the maximum number of matchups for any track was 1741.

For every CloudSat pass over Sweden, its coordinates and time were extracted and the Swerad radar pixels nearest in time and space were selected. If the distance to an observation by CloudSat was larger than 2 km or the difference in time was more than 15 min the data were discarded. Furthermore only CloudSat observations with a confidence flag corresponding to "Moderate" or "High" were analysed. For every CloudSat pass 77–1741 co-located observations were collected. One example of such a pass is shown in Fig. 3. In total 716 545 observational pairs were collected and analysed.

As described in Sect. 2.2 measurements from the ground based radars generally have lower quality far away from the radar station. Figure 2 shows the height above the radar as a function of distance. In order to examine the effect of the varying measure-

AMTD
8, 8157–8189, 2015

Intercomparison of snowfall

L. Norin et al.

ment height we have divided Swerad's measurements into 10 range bins, each containing approximately the same number of measurements (ca 70×10^3). These range bins (0–46, 46–65, 65–82, 82–96, 96–110, 110–125, 125–143, 143–168, 168–199, and > 199 km) are also shown in Fig. 2.

It should be noted that frontal systems, which are mainly responsible for snowfall over Sweden, will advect to varying degree within the maximum 15 min co-location time allowed between CloudSat and Swerad. This is likely to introduce some uncertainty while comparing the snowfall retrievals, especially if any one of the observing system leads or lags the passing front.

3 Results and discussion

In order to get an overview of how the snowfall retrievals from CloudSat and Swerad compare, we first investigated their empirical cumulative distribution functions (ECDF). The ECDF is defined as

$$P(x) = 1 - \int_{x}^{\infty} p(x')\mathrm{d}x' \quad (1)$$

where $p(x)$ is the probability that a measurement has the value x and $P(x)$ is the probability that a measurement has a value equal to or greater than x. In Fig. 4 we show ECDF for the observations made by CloudSat and Swerad. In addition to the ECDF for all distances, Fig. 4 shows the corresponding functions for the various range bins defined in Sect. 2.3.

From Fig. 4 it can be seen that the CloudSat ECDFs are, as expected, unaffected by the distance to the nearest ground-based radar. During all the co-located passes, CloudSat measured snow approximately 10 % of the time. A snowfall rate, S, higher than 0.1 mm h^{-1} was measured less than 5 % of the time. For heavier snowfall, S >

Discussion Paper | Discussion Paper | Discussion Paper | Discussion Paper |

AMTD

8, 8157–8189, 2015

Intercomparison of snowfall

L. Norin et al.

$1\,\mathrm{mm\,h^{-1}}$, a rapid decrease in the frequency of occurrence can be seen. Only 2 ‰ of CloudSat's observations estimated a snowfall rate $S > 1\,\mathrm{mm\,h^{-1}}$.

The ECDFs from Swerad, on the other hand, show a larger variation depending on the distance to the nearest radar. The differences are most clearly seen for light snowfall rates, $S < 0.1\,\mathrm{mm\,h^{-1}}$. The greater the distance to the nearest radar the larger the lowest estimated snowfall rate. The frequency of observed snowfall is also seen to be lower for increasing distances.

At large distances to the nearest radar ($d > 199\,\mathrm{km}$) snowfall was only detected in 1 ‰ of the observations whereas close to the radars ($0 \le d \le 46\,\mathrm{km}$) snow was reported over 10 % of the time. For intermediate snowfall rates, $0.1 \le S \le 1\,\mathrm{mm\,h^{-1}}$, and small to medium distances to the nearest radar, $d < 125\,\mathrm{km}$, the ECDFs of CloudSat and Swerad are similar. However, for large snowfall rates, $S > 1\,\mathrm{mm\,h^{-1}}$, Swerad recorded more frequent and larger snowfall rates compared to CloudSat. The largest snowfall rate was estimated by Swerad to $S \approx 20\,\mathrm{mm\,h^{-1}}$ whereas the largest snowfall rate detected by CloudSat was estimated near $S = 5\,\mathrm{mm\,h^{-1}}$. It is interesting to note that Swerad reported snowfall rates larger than $5\,\mathrm{mm\,h^{-1}}$ for almost all distances to the nearest radar. As non-precipitation echoes (i.e. ground clutter or clear-air returns) are mainly expected to occur close to the radars it seems that these large snowfall rates originate from precipitation and not from clutter. This suggests that either Swerad overestimates the snowfall rate for large reflectivities or that the current 2C-SNOW-PROFILE algorithm may have limited ability to retrieve heavy precipitation.

In Fig. 4 we can further see that, except for short distances to the nearest radar $d < 65\,\mathrm{km}$, CloudSat made more observations of snowfall than Swerad did. This results partly from Swerad overshooting shallow snowfall at large distances and from Swerad's decrease in sensitivity for larger distances.

In order to compare the detection capabilities of each platform, the CloudSat and Swerad matchups were evaluated using the following metrics:

1. probability of detection (POD) for both snowfall and clear conditions,

AMTD
8, 8157–8189, 2015

2. false alarm rate (FAR) for both snowfall and clear conditions,
3. hit rate (HR), and
4. Hanssen–Kuipers skill score (KSS).

These quantities are defined as follows, using the notations in the contingency matrix in Table 2:

$$\mathrm{POD_{snow}} = \frac{d}{c+d} \tag{2}$$

$$\mathrm{POD_{clear}} = \frac{a}{a+b} \tag{3}$$

$$\mathrm{FAR_{snow}} = \frac{b}{b+d} \tag{4}$$

$$\mathrm{FAR_{clear}} = \frac{c}{a+c} \tag{5}$$

$$\mathrm{HR} = \frac{a+d}{a+b+c+d} \tag{6}$$

$$\mathrm{KSS} = \frac{ad-bc}{(a+b)(c+d)} \tag{7}$$

The POD and FAR quantities estimate how efficient the evaluated system is in determining either snow or clear conditions. High values of POD as well as low values of FAR are expected for observational pairs that have a good agreement. The hit rate, HR, measures the efficiency of the evaluated system's ability to correctly classify clear or snowy conditions. As more than 90 % of the co-located observations were of clear weather the HR score is expected to be high, even though the classification of snow might not be as good. The KSS score takes the uneven classification distribution into

AMTD
8, 8157–8189, 2015

account and provides a more balanced measure of how well the evaluated system separated the snow from clear weather. Each scores is calculated for both CloudSat and Swerad using the other observing system as reference.

The lower limit of detectable snowfall, S_{lim}, is ultimately determined by the sensitivity of the radar receiver. For CloudSat the lowest retrieved snowfall rate was $S = 2 \times 10^{-3}\,\text{mm}\,\text{h}^{-1}$ whereas for Swerad the lowest detected snowfall varied between $S = 3 \times 10^{-4}$ and $S = 2 \times 10^{-1}\,\text{mm}\,\text{h}^{-1}$, depending on the distance to the nearest radar (cf. Fig. 4). In order to take the different sensitivities into account, we have calculated the statistical scores using different values for lower limit of detectable snowfall, S_{lim}: 0, 0.01, 0.02, 0.03, 0.05, 0.1, 0.15, 0.25, and $0.35\,\text{mm}\,\text{h}^{-1}$.

Results of the skill scores are shown in Figs. 5 and 6. In Fig. 5 the observations by Swerad are evaluated using CloudSat as reference whereas in Fig. 6 CloudSat is evaluated using Swerad as reference. Every skill score is shown as a function of distance to the nearest ground-based radar as well as a function of S_{lim}. Skill scores were only calculated when at least 150 observations in each category in the contingency matrix existed (cf. Table 2).

In Fig. 5a it is seen that the POD_{snow} ranges from 0.15 to 0.7. The highest values of the POD_{snow} are found for small distances to the nearest ground-based radar, $46 < d < 65\,\text{km}$, together with $0.01 \leq S_{\text{lim}} \leq 0.05\,\text{mm}\,\text{h}^{-1}$. For larger distances the POD_{snow} decreases and for $d > 143\,\text{km}$ approaches 0.1 for all values of S_{lim}. The decreasing values of the POD_{snow} for increasing distances means that either Swerad underestimates the frequency of snowfall or that CloudSat overestimates it. Since the altitude at which Swerad's measurements are made increases with increasing distance (cf. Fig. 2) while CloudSat exhibits a uniform beam height independent of range to the ground radar it is likely that Swerad misses snowfall at large distances due to partial or complete overshooting. Furthermore, the sensitivity of the Swedish radars decreases with increasing distance which would also lead to a decrease in the POD_{snow}, especially for low values of S_{lim}.

AMTD
8, 8157–8189, 2015

In Fig. 5a it is also seen that for increasing distances the POD_{snow} obtains a maximum for increasing values of S_{lim}. This can be understood by examining the ECDFs presented in Fig. 4. The maximum value of the POD_{snow}, for a given distance bin, is found for the value of S_{lim} where the ECDFs of CloudSat and Swerad meet. For example, for $96 < d < 110$ km the ECDFs meet for a snowfall intensity of $0.1\,\mathrm{mm\,h^{-1}}$ and for this value of S_{lim} the POD_{snow} obtains its maximum. For higher values of S_{lim} the POD_{snow} is expected to decrease due to the variability in snowfall intensity in the observations from the evaluated system (Swerad) together with increasing the threshold for snowfall in the reference system (CloudSat).

The POD_{clear}, shown in Fig. 5b, ranges from 0.96 to almost 1. Lower values of the POD_{clear} are only found close to the radar, $d < 46$ km, in combination with $S_{lim} \leq 0.02\,\mathrm{mm\,h^{-1}}$. Close to the ground-based radars Swerad can detect non-precipitation echoes such as ground clutter or returns from clear air targets. It is therefore expected that Swerad occasionally reports false precipitation at these distances. On the other hand, CloudSat can also miss shallow snowfall that forms in its blind zone within 1 km of the surface (Maahn et al., 2014). The POD_{clear} increases for increasing S_{lim}, indicating that this effect is most pronounced for weak echoes or light snowfall.

Figure 5c shows the FAR_{snow} which ranges from 0.1 to 0.55. Except for very small distances to the nearest radar ($d < 46$ km) the FAR_{snow} is seen to increase for increasing values of S_{lim}. This is a result of selecting higher snowfall intensities from the evaluated system (Swerad) together with the variability in intensity of the snowfall observations from the reference system (CloudSat). However, nearest to the ground-based radar, $d < 46$ km, the FAR_{snow} is obtains its minimum for $S_{lim} = 0.1\,\mathrm{mm\,h^{-1}}$. This is again the result of of Swerad reporting echoes from non-precipitation targets in combination with CloudSat missing snowfall in its blind zone.

The FAR_{clear}, shown in Fig. 5d, is low, $FAR_{clear} < 0.04$, close to the nearest ground-based radar indicating that Swerad is good at detecting snowfall at this range. Further from the nearest radar the FAR_{clear} increases up to 0.09 for $S_{lim} = 0\,\mathrm{mm\,h^{-1}}$. However, for $S_{lim} \geq 0.1\,\mathrm{mm\,h^{-1}}$ the $FAR_{clear} < 0.03$ for distances. This confirms the previously discussed suspicion that Swerad misses light snow fall at large distances due to partial overshooting or decreased sensitivity.

The hit rate, HR, is shown in Fig. 5e. The HR is seen to increase for increasing S_{lim}, from HR = 0.91 to HR > 0.98. This occurs because the higher the S_{lim} the more observations are classified as clear by both CloudSat and Swerad. However, a more interesting relation is found as a function of distance to the nearest ground-based radar. Initially the HR increases with distance reaching a maximum value for $46 < d < 82$ km beyond which it decreases monotonically. This result represents a combination of the previously discussed problems occurring close (non-precipitation echoes detected by Swerad and blind zone for CloudSat) and far (overshooting and decreased sensitivity by Swerad) from the nearest ground-based radar. The distance where HR obtains its maximum shows the optimum distance when comparing the intensity estimates from both systems. Referring to Fig. 2, it is encouraging to note that the radar beam is at an altitude of about 1 km at this range from the radar coinciding with the height to which the CloudSat observations correspond.

Figure 5f shows the Hanssen–Kuipers skill score, KSS. This score varies between 0.15 < KSS < 0.7. The lowest values of the KSS are found for large distances from the nearest ground-based radar, reflecting the low values of the $\mathrm{POD}_{\mathrm{snow}}$ seen in Fig. 5a. The highest values of the KSS are found for small to moderate distances to the nearest radar ($46 < d < 65$ km) together with low to moderate lower limits of the snowfall rate ($0.01 \leq S_{\mathrm{lim}} \leq 0.05\,\mathrm{mm\,h^{-1}}$). This shows the distances and the values of S_{lim} for which the observations from the measurement systems agree best, when using CloudSat as reference.

In Fig. 6 the same set of skill scores is shown but now using Swerad as the reference. However, not all skill scores are independent of each other. From the definitions of the skill scores (see Eqs. 2–7) and the contingency matrix (cf. Table 2) it can be seen that $\mathrm{POD}_{\mathrm{snow/clear}}$ (using CloudSat/Swerad as reference) is equal to 1-$\mathrm{FAR}_{\mathrm{snow/clear}}$ (using Swerad/CloudSat as reference).

Discussion Paper | Discussion Paper | Discussion Paper | Discussion Paper |

AMTD

8, 8157–8189, 2015

Intercomparison of snowfall

L. Norin et al.

The POD_{snow} is shown in Fig. 6a. For low to moderate lower limits of the snowfall rate, $0 \leq S_{lim} = 0.1\,\mathrm{mm\,h^{-1}}$, the POD_{snow} ranges from 0.6 to 0.9 whereas for high lower limits of the snowfall rate, $S_{lim} \geq 0.4\,\mathrm{mm\,h^{-1}}$, the POD_{snow} decreases down to almost 0.45. The decreasing values of the POD_{snow} for increasing values of S_{lim} are explained by the variability in the snowfall intensity of the evaluated system (CloudSat) together with the increasing threshold for snowfall of the reference system (Swerad). Close to the radars, $d < 46$ km, CloudSat underestimates the frequency of snowfall reported by Swerad more than for larger distances, for $S_{lim} \leq 0.1\,\mathrm{mm\,h^{-1}}$. This was also seen in Fig. 5b and is contributed to a combination of CloudSat missing shallow snowfall in its blind zone and Swerad reporting non-precipitation echoes.

The POD_{clear}, shown in Fig. 6b, is very high, close to 1, except for $d > 82$ km in combination with $S_{lim} \leq 0.01\,\mathrm{mm\,h^{-1}}$ where $POD_{clear} < 0.94$. The lower values of the POD_{clear} are, as previously discussed, explained by Swerad missing or partially overshooting snowfall at large distances together with Swerad's decreased sensitivity for larger distances.

The FAR_{snow}, see Fig. 6c, ranges from 0.3 to 0.9. The FAR_{snow} is low close to the radars, $d < 82$ km, together with $S_{lim} \leq 0.1\,\mathrm{mm\,h^{-1}}$ indicating good agreement between the observing systems. For larger distances to the nearest ground-based radar the values of FAR_{snow} decrease as a result of Swerad missing snowfall due to overshooting and decreased sensitivity.

It can further be seen that for increasing distances the minimum value of the FAR_{snow} is found for increasing values of S_{lim}. This can again be explained by a combination of Swerad missing observations of snowfall due to overshooting and decreased sensitivity and the variability in snowfall intensity in the observations from the reference system (Swerad) together with a increasing the threshold of snowfall for the evaluated system (CloudSat).

Figure 6d shows the FAR_{clear} which is almost zero everywhere, meaning that when CloudSat reports clear weather Swerad almost never reports snow. Higher values, $FAR_{clear} > 0.02$ are only found close to the nearest ground-based radar, $d < 65$ km,

AMTD
8, 8157–8189, 2015

and for $S_{lim} \leq 0.03\,mm\,h^{-1}$. The higher values of the FAR_{clear} confirm the previous observation that for these distances CloudSat measures snow less often than Swerad, due to CloudSat's blind zone and Swerad reporting non-precipitation echoes. Even very close to the nearest radar, $d < 46$ km, the FAR_{clear} approaches zero for increasing values of S_{lim} suggesting that CloudSat predominantly underestimates light snowfall near the radars.

The hit rate, shown in Fig. 6e, is reproduced for convenience but is exactly the same as the hit rate shown in Fig. 5e since HR is symmetric with respect to the choice of reference. The KSS, however, differs depending on which system is used as reference. The KSS using Swerad as reference is shown in Fig. 6f. This score varies between $0.4 < KSS < 0.8$. The lowest values of the KSS are found for high values of the lower limit of the snowfall rate limit, $S_{lim} \geq 0.25\,mm\,h^{-1}$, which reflects the corresponding low values of the POD_{snow} (cf. Fig. 6a). For the highest value of the lower limit of the snowfall rate, $S_{lim} = 0.35\,mm\,h^{-1}$, the KSS decreases for all distances and attains values between 0.4 and 0.6. High values of the KSS are found for intermediate distances to the nearest radar ($46 < d < 143$ km) together with $S_{lim} \leq 0.03\,mm\,h^{-1}$. This is a result of the corresponding high values of the POD_{snow}. This shows again that an optimum range to the nearest ground-based radar exist where the problems close to (non-precipitation echoes from Swerad and CloudSat's blind zone) and far from (Swerad's decreased sensitivity and beam overshooting) the radars are minimised.

It is worth noting that these skill scores are very good demonstrative examples as to why we need to alternate the observing system used as the reference. The impact of their different sensitivities, observational capabilities, and statistical artefacts resulting from these differences, are clearly visible in the two sets of skill scores presented in Figs. 5 and 6.

The co-located observational pairs from CloudSat and Swerad are further analysed using 2-D probability density functions (PDFs) in Fig. 7 which shows all observations when both CloudSat and Swerad reported snow.

AMTD
8, 8157–8189, 2015

Ideally all co-located pairs should lie on the line of equality, but in reality, due to different sensitivities and observing principles, some scatter is expected. In order to provide an objective measure of the agreement between the observational pairs x_i and y_i a simple metric, based on the normalised minimum distance of all N observational pairs to the line of equality, was defined.

$$m = 1 - \frac{1}{N}\sum_{i=1}^{N}\frac{\sqrt{(x_i - y_i)^2}}{x_i + y_i} \tag{8}$$

where $0 \leq m \leq 1$ and $m = 1$ corresponds to all observational pairs lying on the line of equality.

In Fig. 7a the 2-D PDF for all observational pairs is shown. It can be seen that the most frequently observed snowfall rates were estimated to $S < 0.1\,\mathrm{mm\,h^{-1}}$ for both CloudSat and Swerad. The general agreement between the measurement systems is good, $m = 0.59$, and the agreement is even better for snowfall rates $S > 0.1\,\mathrm{mm\,h^{-1}}$. For light snowfall rates, $S < 0.05\,\mathrm{mm\,h^{-1}}$, Swerad tends to estimate slightly lower snowfall rates than CloudSat.

As shown in Fig. 4, the snowfall retrievals from Swerad are sensitive to the distance from the radar station. In order to investigate sensitivity to this distance, Fig. 7b–k show the 2-D PDFs for all observational pairs for different distances to the nearest ground based radar (cf. Sect. 2.3 and Fig. 4). In Fig. 7b we see that close to the radar, $d < 46\,\mathrm{km}$, the agreement between CloudSat and Swerad is good, $m = 0.59$. Very low snowfall rates, $S < 0.05\,\mathrm{mm\,h^{-1}}$, tend to be estimated somewhat lower by Swerad. The same tendency is also seen for the next distance bin, $46 < d < 65\,\mathrm{km}$, shown in Fig. 7c but for this range to the nearest radar the overall agreement is higher, $m = 0.61$.

In Fig. 7d–k it is seen that for increasing distance to the nearest radar, Swerad observes fewer and fewer light snowfall events (cf. Fig. 4). This is likely a result of Swerad's decreased sensitivity with increasing distance and by partial beam overshooting of the snowfall, discussed in Sects. 2.2 and 3. The agreement metric is seen to decrease from $m = 0.62$ to $m = 0.49$ (with the exception of slightly higher scores, $m = 0.55$

AMTD
8, 8157–8189, 2015

and $m = 0.53$, for Fig. 7j and k). However, for snowfall rates $0.1 \leq S \leq 1\,\mathrm{mm\,h^{-1}}$ the agreement remains good, regardless of distance.

4 Conclusions

In the present study, we exploited data from the Swedish ground based radar network (Swerad) and the Cloud Profiling Radar onboard the CloudSat satellite (2C-SNOW-PROFILE) to provide insights into their performance in snowing scenes. The different sensitivities and observing principles of these two systems offer increased understanding of their strengths and limitations. Furthermore, the high latitude geographical location of Sweden allows us to sample and intercompare snowfall retrievals under different meteorological and surface conditions than previously reported. In total, more than 7.2×10^5 co-located observations were evaluated from 1 January 2008 till 31 December 2010, except during summer months.

The intercomparison shows encouraging agreement between the two observing systems. The distributions of snowfall rates are similar for CloudSat and Swerad for the range between 0.1 and $1.0\,\mathrm{mm\,h^{-1}}$. The results from the sensitivity studies indicate that the best agreement is observed when CloudSat passes close to a Swerad station (46–82 km), when the observational conditions for both systems are comparable. Larger disagreements outside this range suggest that both platforms have difficulty with shallow snow but for different reasons. A clear tendency is observed for the correlation between Swerad and CloudSat to degrade with increasing distance from the nearest Swerad station. This mainly occurs due to Swerad's decreased sensitivity for increasing distances but also as Swerad systematically overshoots low level precipitating systems further away from the station, leading to underestimation of snowfall rate and occasionally missing the precipitation altogether. Data pairs close to the radar, on the other hand, suggest that CloudSat likely misses some shallow snow events, due to ground clutter, that are detected by the ground-based radars.

AMTD
8, 8157–8189, 2015

We further investigated various statistical metrics, such as the probability of detection, false alarm rate, hit rate, and the Hanssen–Kuipers skill scores, and the sensitivity of these metrics to snowfall rate and the distance from the radar station. All evaluated metrics also show a clear tendency that the scores degrade with increasing distance from the Swerad stations. A closer inspection of observations shows that 2C-SNOW-PROFILE has limited ability to retrieve at the higher end of snowfall intensity distribution (> 1 $\mathrm{mm\,h^{-1}}$) causing deviation from the corresponding distribution from Swerad. On the lower end of the distribution, both observing systems seem to suffer from limitations. While Swerad detects non-precipitating, low intensity echoes closest to the stations that are often misclassified as light snowfall, CloudSat/CPR is also affected by the so-called blind zone where its sensitivity is reduced considerably in the lowermost kilometre from the surface. These limitations make comparison of light snowfall events difficult and impractical.

Finally, it should be mentioned here that although the design purpose and end users of these two observing systems are different, such inter-comparisons help assess the performance of ground-based systems for weather applications, while also providing uncertainty information for climate applications that use satellite products (Boening et al., 2012; Palerme et al., 2014). The fact that Swerad and CloudSat/CPR broadly agree with one another in the 0.1–1.0 $\mathrm{mm\,h^{-1}}$ intensity range, recorded by the majority of snowfall events, could be exploited in future studies to reconcile differences between these two systems and in particular to improve statistical relationship between reflectivity and snowfall rate derived from ground based radars. Our preliminary comparison of snowfall distributions employing various Z–S relationships shows that there exists a large room for improvements of Swerad data. Formulating a representative Z–S relationship has been one of the chronic problems, often discussed widely in the scientific community. CloudSat with its uniform calibration and beam height (together with information on cloud microphysics) has potential to be a realistic reference in this context.

Acknowledgements. The portion of this research by T. S. L'Ecuyer, N. B. Wood, and M. Smalley were performed at the University of Wisconsin-Madison and at Colorado State University for

AMTD
8, 8157–8189, 2015

the Jet Propulsion Laboratory, California Institute of Technology, sponsored by the National Aeronautics and Space Administration CloudSat program.

References

Battan, L. J.: Radar Observation of the Atmosphere, University of Chicago Press, Chicago, 324 pp., 1973. 8165

Bech, J., Codina, B., Lorente, J., and Bebbington, D.: The sensitivity of single polarization weather radar beam blockage correction to variability in the vertical refractivity gradient, J. Atmos. Ocean. Tech., 20, 845–855, doi:10.1175/1520-0426(2003)020<0845:TSOSPW>2.0.CO;2, 2003. 8165

Boening, C., Lebsock, M., Landerer, F., and Stephens, G.: Snowfall-driven mass change on the East Antarctic ice sheet, Geophys. Res. Lett., 39, L21501, doi:10.1029/2012GL053316, 2012. 8177

Cao, Q., Hong, Y., Chen, S., Gourley, J. J., Zhang, J., and Kirstetter, P. E.: Snowfall detectability of NASA's CloudSat: the first cross-investigation of its 2c-snow-profile product and national multi-sensor mosaic QPE (NMQ) snowfall data, Prog. Electromagn. Res., 148, 55–61, doi:10.2528/PIER14030405, 2014. 8160, 8161

Carlsson, I.: NORDRAD – weather radar network, in: COST 75 Weather Radar Systems, edited by: Collier, C. G., European Commission, Luxembourg, 45–52, 1995. 8164

Devasthale, A. and Norin, L.: The large-scale spatio-temporal variability of precipitation over Sweden observed from the weather radar network, Atmos. Meas. Tech., 7, 1605–1617, doi:10.5194/amt-7-1605-2014, 2014. 8161

Doviak, R. J. and Zrnić, D. S.: Doppler Radar and Weather Observations, 2 edn., Dover Publications, Mineola, New York, 2006. 8164

Häggmark, L., Ivarsson, K.-I., Gollvik, S., and Olofsson, P.-O.: Mesan, an operational mesoscale analysis system, Tellus A, 52, 2–20, doi:10.1034/j.1600-0870.2000.520102.x, 2000. 8165

Haynes, J. M., L'Ecuyer, T. S., Stephens, G. L., Miller, S. D., Mitrescu, C., Wood, N. B., and Tanelli, S.: Rainfall retrieval over the ocean with spaceborne W-band radar, J. Geophys. Res., 114, D00A22, doi:10.1029/2008JD009973, 2009. 8162

Kulie, M. and Bennartz, R.: Utilizing spaceborne radars to retrieve dry snowfall, J. Appl. Meteorol., 48, 2564–2580, doi:10.1175/2009JAMC2193.1, 2009. 8160

L'Ecuyer, T. S. and Jiang, J.: Touring the atmosphere aboard the A-Train, Phys. Today, 63, 36–41, 2010. 8160

Levizzani, V., Laviola, S., and Cattani, E.: Detection and measurement of snowfall from space, Remote Sensing, 3, 145–166, doi:10.3390/rs3010145, 2011. 8159, 8160

Liu, G.: Deriving snow cloud characteristics from CloudSat observations, J. Geophys. Res., 113, D00A09, doi:10.1029/2007JD009766, 2008. 8160

Liu, G. and Seo, E. K.: Detecting snowfall over land by satellite high-frequency microwave observations: the lack of scattering signature and a statistical approach, J. Geophys. Res.-Atmos., 118, 1376–1387, doi:10.1002/jgrd.50172, 2013. 8160

Liu, X. and Yanai, M.: Influence of Eurasian spring snow cover on Asian summer rainfall, Int. J. Climatol., 22, 1075–1089, doi:10.1002/joc.784, 2002. 8159

Maahn, M., Burgard, C., Crewell, S., Gorodetskaya, I. V., Kneifel, S., Lhermitte, S., Van Tricht, K., and Van Lipzig, N. P. M.: How does the spaceborne radar blind zone affect derived surface snowfall statistics in polar regions?, J. Geophys. Res.-Atmos., 119, 13604–13620, doi:10.1002/2014JD022079, 2014. 8161, 8171

Michelson, D.: The Swedish weather radar production chain, in: Proceedings of the Fourth European Conference on Radar in Meteorology and Hydrology, Barcelona, Spain, 18–22 September 2006, 382–385, ERAD, 2006. 8161, 8165

Michelson, D. B. and Koistinen, J.: Gauge-radar network adjustment for the Baltic Sea Experiment, Phys. Chem. Earth Pt. B, 25, 10–12, 2002. 8161, 8165

Michelson, D. B., Andersson, T., Koistinen, J., Collier, C. G., Riedl, J., Szturc, J., Gjertsen, U., Nielsen, A., and Overgaard, S.: BALTEX Radar Data Centre Products and their Methodologies, Reports Meteorology and Climatology RMK 90, SMHI, 2000. 8161

Noh, Y. J., Liu, G., Jones, A. S., and Vonder Haar, T. H.: Toward snowfall retrieval over land by combining satellite and in situ measurements, J. Geophys. Res.-Atmos., 114, D24205, doi:10.1029/2009JD012307, 2009. 8160

Palerme, C., Kay, J. E., Genthon, C., L'Ecuyer, T., Wood, N. B., and Claud, C.: How much snow falls on the Antarctic ice sheet?, The Cryosphere, 8, 1577–1587, doi:10.5194/tc-8-1577-2014, 2014. 8177

Rodgers, C.: Inverse Methods for Atmospheric Sounding, World Scientific Publishing, Singapore, 2000. 8162

AMTD
8, 8157–8189, 2015

Skofronick-Jackson, G. M., Johnson, B. T., and Munchak, S. J.: Detection thresholds of falling snow from satellite-borne active and passive sensors, IEEE T. Geosci. Remote, 51, 4177–4189, doi:10.1109/TGRS.2012.2227763, 2012. 8161

Smalley, M., L'Ecuyer, T., Lebsock, M., and Haynes, J.: A comparison of precipitation occurrence from the NCEP StageIV QPE Product and the CloudSat Cloud Profiling Radar, J. Hydrol., 15, 444–458, doi:10.1175/JHM-D-13-048.1, 2014. 8160

Surussavadee, C. and Staelin, D. H.: Satellite retrievals of Arctic and equatorial rain and snowfall rates using millimeter wavelengths, IEEE T. Geosci. Remote, 47, 3697–3707, doi:10.1109/TGRS.2009.2029093, 2009. 8160

Tanelli, S., Durden, S. L., Im, E., Pak, K. S., Reinke, D. G., Partain, P., Haynes, J. M., and Marchand, R. T.: CloudSat's Cloud Profiling Radar after two years in orbit: performance, calibration, and processing, IEEE Trans. Geosci. Remote, 46, 3560–3573, 2008. 8162

Turner, A. G. and Slingo, J. M.: Using idealized snow forcing to test teleconnections with the Indian summer monsoon in the Hadley Centre GCM, Clim. Dynam., 36, 1717–1735, doi:10.1007/s00382-010-0805-3, 2011. 8159

Waliser, D. E., Li, J.-L. F., L'Ecuyer, T. S., and Chen, W.-T.: The impact of precipitating ice and snow on the radiation balance in global climate models, Geophys. Res. Letters, 38, L06802, doi:10.1029/2010GL046478, 2011. 8159

Wood, N. B.: Estimation of snow microphysical properties with application to millimeter-wavelength radar retrievals for snowfall rate, PhD thesis, Colorado State University, Fort Collins, Colorado, available at: http://hdl.handle.net/10217/48170 (last access: 3 August 2015), 2011. 8160, 8162

Wood, N. B., L'Ecuyer, T., Vane, D. G., Stephens, G. L., and Partain, P.: Level 2C snow profile process description and interface control document, Tech. rep., Colorado State University, available at: http://www.cloudsat.cira.colostate.edu/sites/default/files/products/files/2C-SNOW-PROFILE_PDICD.P_R04.20130210.pdf (last access: 3 August 2015), 2013. 8160, 8162

Wood, N. B., L'Ecuyer, T. S., Heymsfield, A. J., and Stephens, G. L.: Microphysical constraints on millimeter-wavelength scattering properties of snow particles, J. Appl. Meteorol. Clim., 54, 909–931, doi:10.1175/JAMC-D-14-0137.1, 2015. 8162

Ye, H., Bao, Z., and Feng, X.: Connections of Siberian snow onset dates to the following summer's monsoon conditions over Southeast Asia, Int. J. Climatol., 25, 1567–1584, doi:10.1002/joc.1201, 2005. 8159

Table 1. Selected characteristics of Swedish weather radars.

Tilt angles	0.5, 1.0, 1.5, 2.0°	2.5, 4.0, 8.0, 14.0, 24.0, 40.0°
Transmit power	250 kW	250 kW
Wavelength	5.35 cm	5.35 cm
Gain	44.7 dB	44.7 dB
Pulse width	0.5 µs	0.5 µs
Beam width	0.9°	0.9°
PRFs	600/450 Hz	1200/900 Hz
Rotational speed	2 rpm	2 rpm
Measurement radius	240 km	120 km
Radial resolution	2 km	1 km
Azimuthal resolution	0.86°	0.86°
Range cells	120	120
Azimuth gates	420	420
Max unambiguous velocity	24 m s^{-1}	48 m s^{-1}

AMTD
8, 8157–8189, 2015

Intercomparison of snowfall

L. Norin et al.

Table 2. Contingency matrix for observations from CloudSat and Swerad.

		Evaluated	
	Scenario	Clear	Snow
Reference	Clear	*a*	*b*
	Snow	*c*	*d*

AMTD
8, 8157–8189, 2015

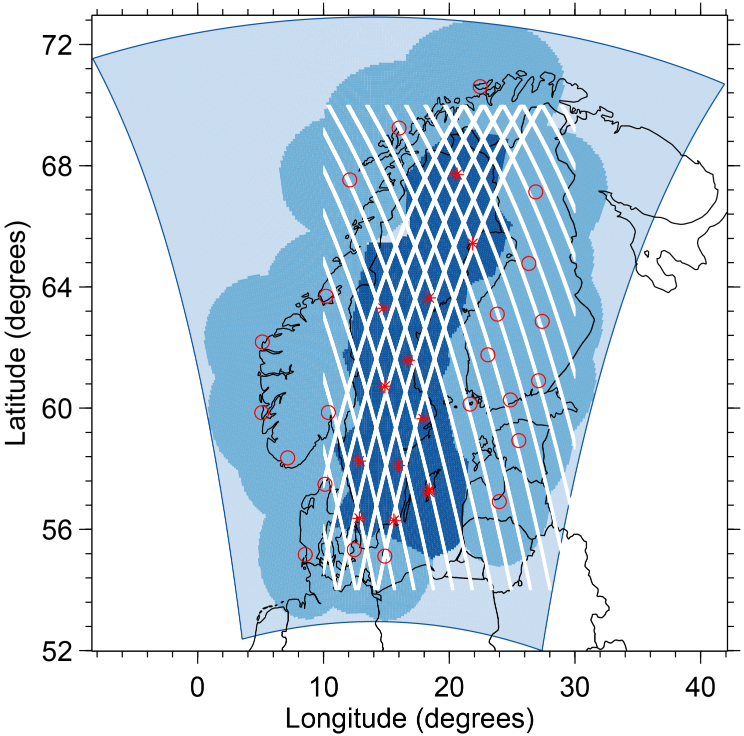

Figure 1. Area covered by the Nordrad composite (light blue). Coverage by all Nordic radars is shown in blue. Data originating from Swedish radars (Swerad) are displayed in dark blue. The positions of the Swedish radars are depicted by red stars whereas the locations of the other radars are shown by red circles. Tracks of the selected CloudSat passes are illustrated by white lines.

AMTD
8, 8157–8189, 2015

Title Page
Abstract | Introduction
Conclusions | References
Tables | Figures
◀| |▶
◀ ▶
Back | Close
Full Screen / Esc
Printer-friendly Version
Interactive Discussion

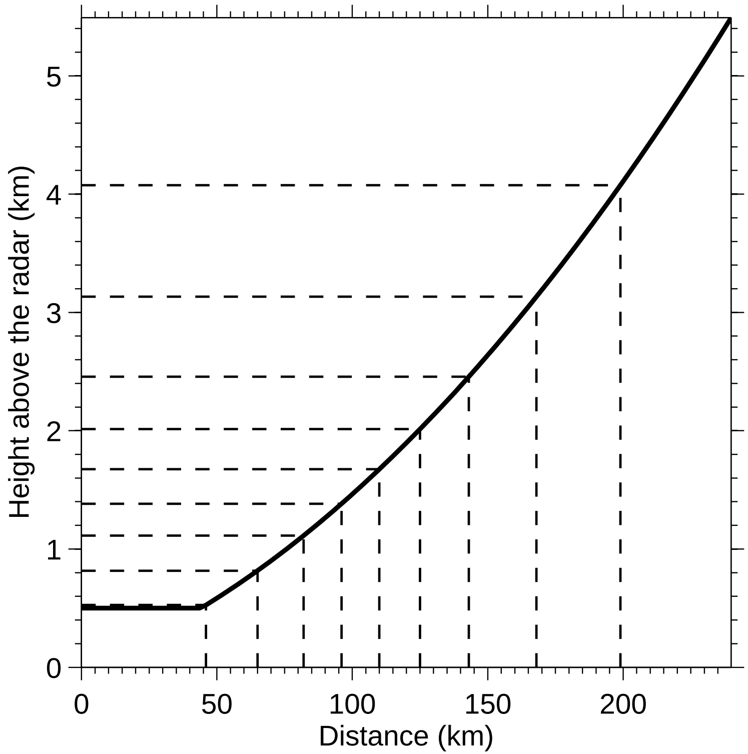

Figure 2. Measurement height as a function of distance for Swerad (thick, solid line). Thin, dashed lines show the range limits that were used to divide the Swerad data into 10 range bins with an equal number of observations (0–46, 46–65, 65–82, 82–96, 96–110, 110–125, 125–143, 143–168, 168–199, and > 199 km).

AMTD
8, 8157–8189, 2015

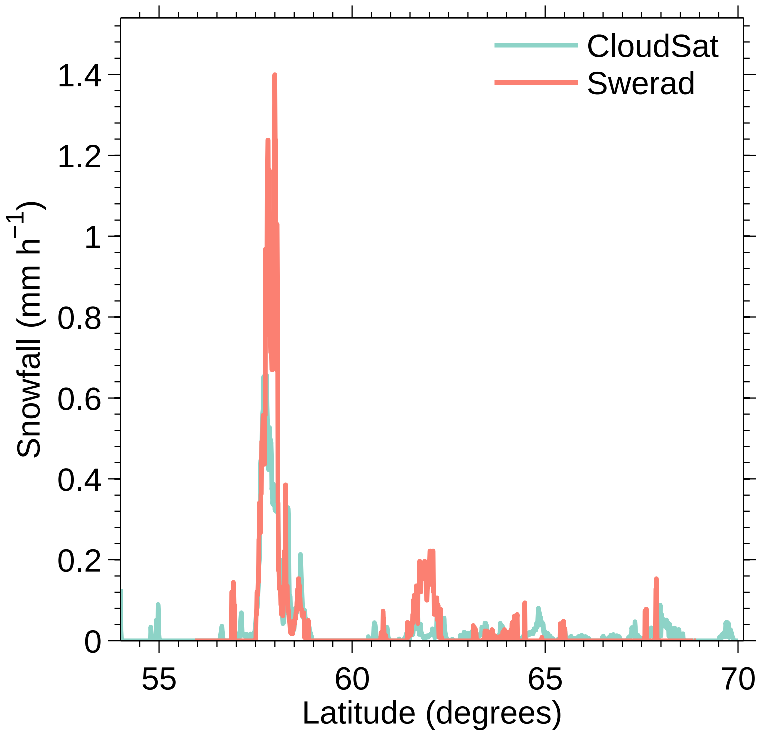

Figure 3. An example of a time series of co-located snowfall rate observations made by CloudSat and Swerad.

AMTD
8, 8157–8189, 2015

Intercomparison of snowfall

L. Norin et al.

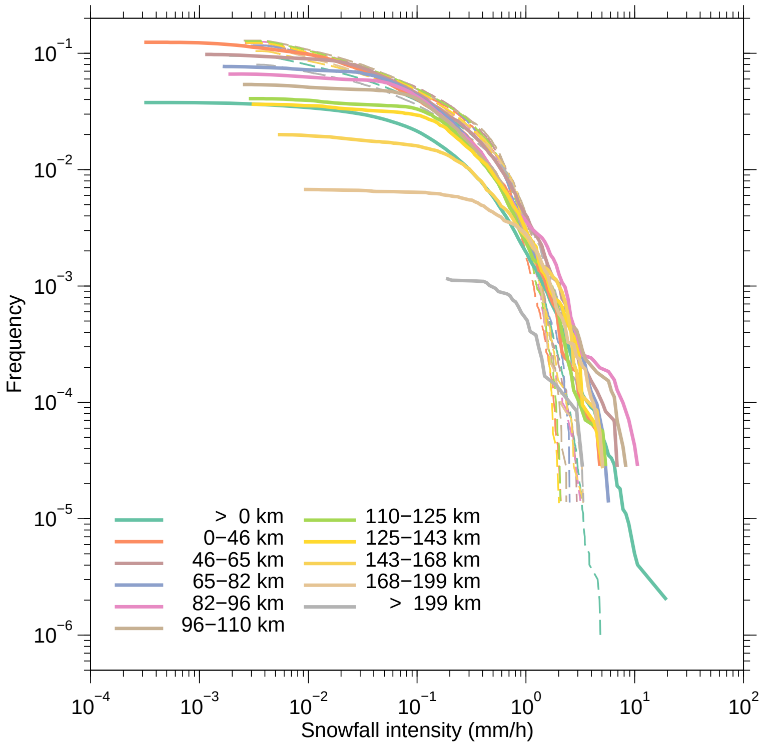

Figure 4. Empirical cumulative distribution functions for observations of snowfall intensities from Swerad (solid lines) and CloudSat (dashed lines), for various distances to the nearest ground-based radar.

AMTD
8, 8157–8189, 2015

Intercomparison of snowfall

L. Norin et al.

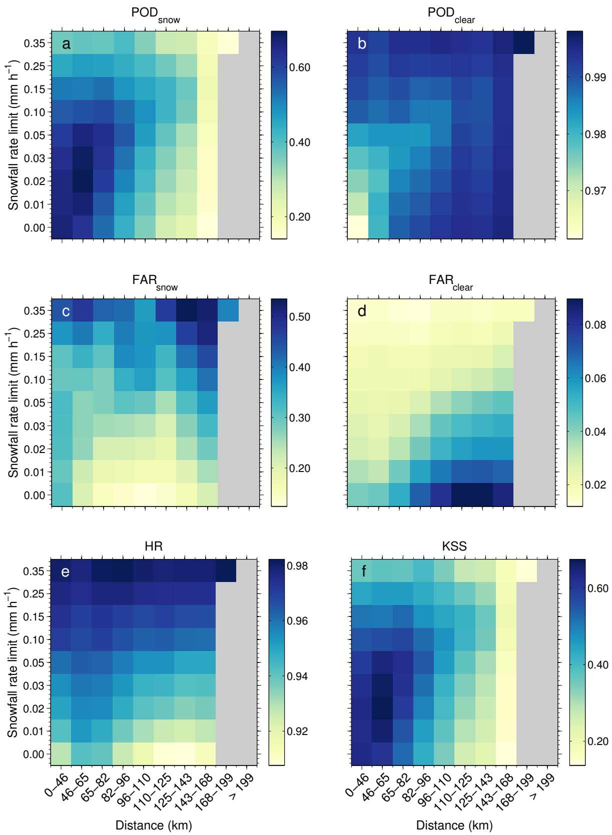

Figure 5. Statistical scores for Swerad using CloudSat as reference. The scores are shown as a function of distance to the nearest radar as well as for different lower limits of the snowfall rate. The panels show the probability of detecting snow **(a)**, the probability of detecting clear weather **(b)**, false alarm rate of snow **(c)**, false alarm rate of clear weather **(d)**, hit rate **(e)**, and the Hanssen–Kuipers skill score **(f)**.

AMTD
8, 8157–8189, 2015

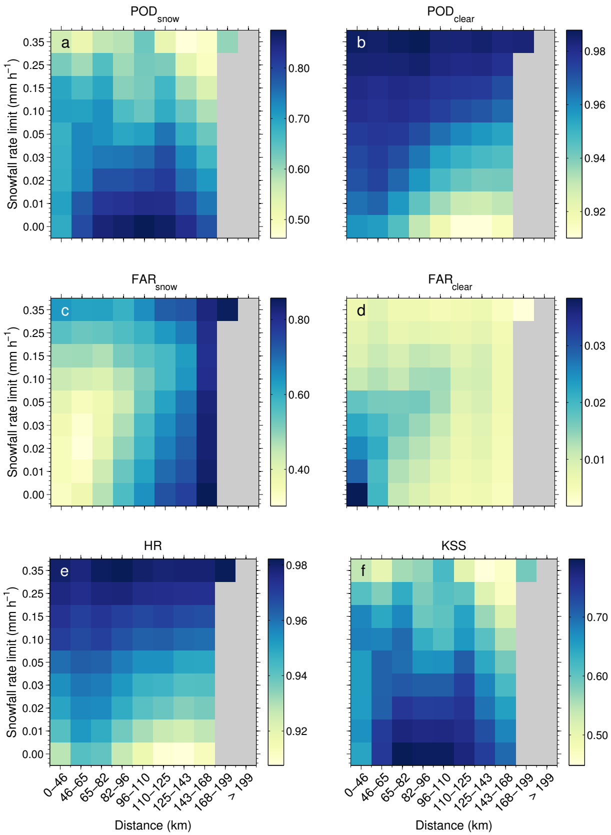

Figure 6. Statistical scores for CloudSat using Swerad as reference. The scores are shown as a function of distance to the nearest radar as well for different lower limits of the snowfall rate. The panels show the probability of detecting snow **(a)**, the probability of detecting clear weather **(b)**, false alarm rate of snow **(c)**, false alarm rate of clear weather **(d)**, hit rate **(e)**, and the Hanssen–Kuipers skill score **(f)**.

AMTD
8, 8157–8189, 2015

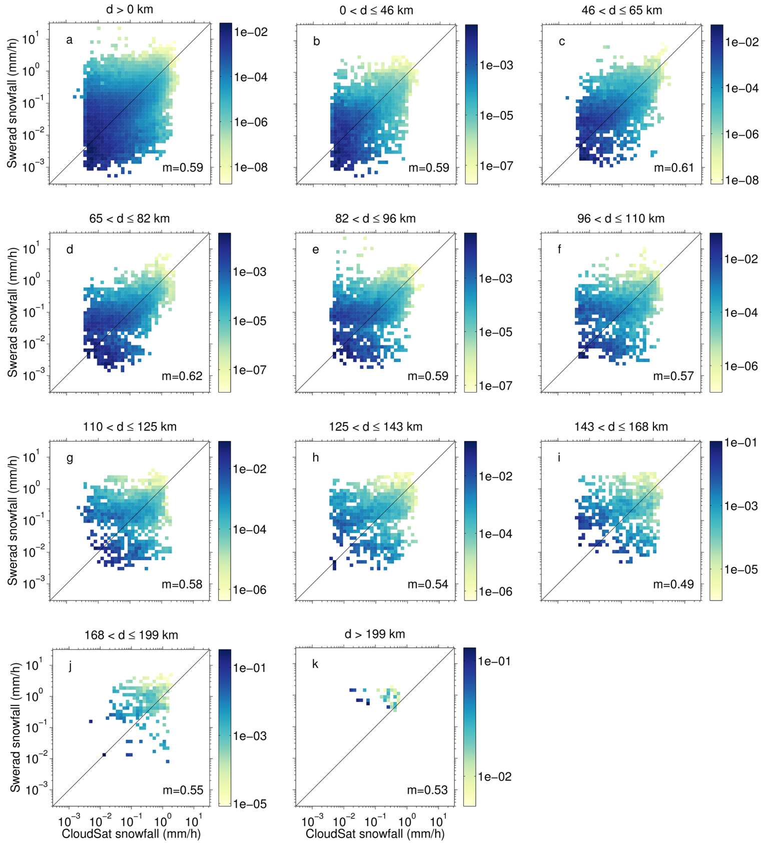

Figure 7. 2-D probability density functions (PDFs) of observational pairs of snowfall by CloudSat and Swerad. Panel **(a)** shows the 2-D PDF for all observational pairs whereas panels **(b–k)** show the 2-D PDF for various distances to the nearest ground-based radar. Note the logarithmic scales. The metric m estimates how well the observations agree ($0 \le m \le 1$ where $m = 1$ is perfect agreement).

AMTD
8, 8157–8189, 2015

Intercomparison of snowfall

L. Norin et al.